Open Access
Baghdad Science Journal **Vol.16 (4) Supplement 2019**

DOI: http://dx.doi.org/10.21123/bsj.2019.16.4(Suppl.).1036

Structural and Optical Properties for Nanostructure (Ag_2O/Si & Psi) Films for Photodetector Applications

Intisar Abbas Hamad [1*] ***Rana Ismael Khaleel*** [2] ***Asmaa Mohmmed Raoof*** [3]

Received 25/9/2018, Accepted 9/5/2019, Published 18/12/2019

Abstract:

Ag_2O (Silver Oxide) is an important p-type (in chasm to most oxides which were n-type), with a high conductivity semiconductor. From the optical absorbance data, the energy gap value of the Ag_2O thin films was 1.93 eV, where this value substantially depends on the production method, vacuum evaporation of silver, and optical properties of Ag_2O thin films are also affected by the precipitation conditions. The n-type and p-type silicon substrates were used with porous silicon wafers to precipitate ±125 nm, as thick Ag_2O thin film by thermal evaporation techniques in vacuum and via rapid thermal oxidation of 400°C and oxidation time 95 s, then characterized by measurement of XRD, optical properties and scanning electron microscopy properties (SEM). Maximum value of photo response obtained from p-Ag_2O/p-PS/Si photodetector results revealed two peak sat 600 nm and 800 nm. According to the x-ray diffraction four peaks appear, (111), (200), (110) and (311) Ag, respectively, (polycrystalline film) and lattice constant of (4.077 Å). Also the results showed a sharp increasing in the absorption-wave length plot of Ag_2O film at UV and IR regions. The accumulation of the stars-like are semi-regular of the Ag_2O nanocrystals on the surface of p-type PS and the other diffuse inside the pores in a nearly uniform distribution with a different grain size on the surface. The results of the dislocation density and strain are decreased with the grain size increasing.

Key words: Ag_2O, Porous silicon, Structural study, Spectral Responsivity, Thermal evaporation system in vacuum .

Introduction:

Silver being diverse forms and various phases like Ag_2O, AgO, Ag_3O_4 and Ag_2O_3, belong to a group of inorganic materials (1-4). Experimentally, the workers found that Ag_2O,and AgO are the most important forms in observable phases than silver oxide multivalent (Ag_3O_4, Ag_2O_3) and exhibited a high specific capacity(2,3).Several authors (5,6)have examined the preparation and properties of silver and silver oxide thin films using a variety of techniques such as radio frequency magnetron sputtering, vapor-liquid-solid process, and a spray pyrolysis method, etc. (the value of the optical band gap of Ag_2O strongly depends on the preparation method).

The objective of this work is to produce the nanocrystalline silver oxide films by means of thermal evaporation techniques in vacuum and via rapid thermal oxidation of 400°C and oxidation time 95 s, for Ag precipitated film on n-type and p-type wafers Si and porous Si(where the porous silicon is an affective material in optoelectronics filed due to its high absorption coefficient, low cost, simple synthesis technique and good anti-reflection coating (7,8), prepared by electrochemical etching and characterized via of XRD, SEM and optical measurement towards its application as photo detectors, physical and chemical properties of silver and silver oxide are illustrated in Table1.

[1] Physics Department, College of Science for Women, University of Baghdad, Baghdad, Iraq
[2] Physics Department, College of Science, Al-Mustansiriyah University, Baghdad, Iraq
[3] 3Physics Department, College of Education, Al-Mustansiriyah University, Baghdad, Iraq.
[*]Corresponding author: warda983@yahoo.com

Table 1. physical and chemical properties of (Ag) and (Ag_2O) (9) .

symbol	Crystal structure	Color	Melting point ^oC	Density kg/m^3	Molecular weight kg/mol	Lattice constant
Ag	FCC	Silver	1234.93	7220	0.107	4.077
Ag_2O	Pyramid-like	Brown -black	460	7220	0.231	4.736

Materials and Methods:

Silver thin films were deposited using thermal evaporation system, high purity (99.9%) silver on a clean glass slide substrate (2x2cm) at (±125nm) measured by electric balance as a thickness and crystalline wafer of p and n-type at room temperature with resistivity of (0.2-2) Ω.cm, under low pressure (~10^{-6} torr), thickness about (507 µm) prepared using a rectangles wire-cut machine with areas of (1.7×1.7) cm^2. P-type Ag_2O thin film highly (111) oriented was prepared using rapid thermal oxidation system (RTO) with oxidation time 95 s, as shown in Fig. 1-a. Electrochemical etching , (anodization etching, in dark) for p-type Si wafer, while n-type was etched by using (PECE),with halogen lamp (100 W) to produce porous Si (PSi) layers, performed at room temperature with HF (40%) and high purity Ethanol in (1:1) mixture using Au electrode with 23mA/cm^2 applied current density for 15min for the nano size formation process where the etched area was (0.805 cm^2), the previously procedure is shown in the Fig.1-b. After that, thickness of 0.1 µm of Al layers were deposited on the backsides of the Ag_2O films using the evaporation technique which deposited on Si and Psi wafers. Photovoltaic measurements of hetero junctions were estimated. Ag_2O thin films were characterized by the measurement of XRD(LabX XRD 6000 SHIMADZU X-Ray diffractometer with Cu Kα radiation, wavelength 1.54059 Å, voltage 30 kV, current 15 mA, scanning speed = 4°/min), optical properties and scanning electron microscopy properties SEM (carried out by VEGA TESCAN-SEM at 20–30 kV).

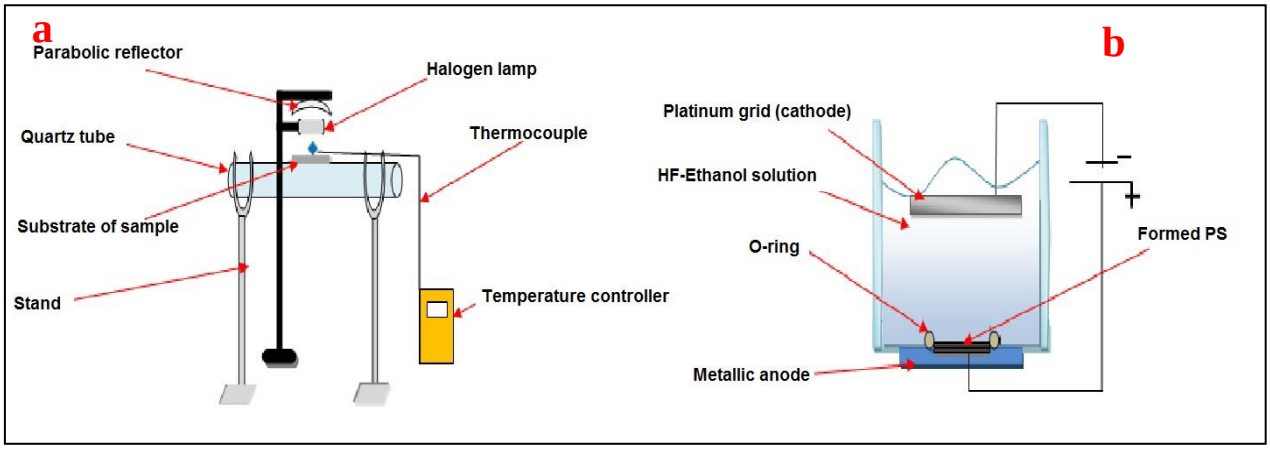

Figure 1. (a) Rapid thermal Oxidation (RTO) Setup (10) (b) Schematic diagram (single tank vertical cell) of the electrochemical etching set –up (1).

Results and Discussion:

Structural Characterization of Ag_2O Thin Film:-

The structure and lattice parameters of Ag thin films Fig. 2-a and Ag_2O nanostructure films Fig.2-b were analyzed by X-Ray diffractometer which contains main peaks at diffraction angle of 32.784^o and 38.6156^o corresponds to (111) and (101) planes with lattice constant 4.736A^o. The two diffraction peaks are indexed to the pyramid - like structure and there is no trace of cubic face, which has a well matching with standard peaks (JCPDS No. 77-2307) (11,12). The sharpness of the peak appears at (111) plane mention that the crystal characteristic of the Ag_2O thin film amelioration with raising the oxidation temperature as shown in Fig. 2-b and listed in Table 2. Also, the crystalline quality of Ag_2O is greatly enhanced with smaller width of the peaks (13) and a strong diffraction planes have been taken from the same table accounts, four peaks has been appeared.

The film is polycrystalline according to the ASTM standards where (111), (200), (110) and (311) Ag, respectively, with lattice constant of 4.077 Å could be recognized. This was related to the formation of Ag thin film and such result indicates that no formation of the oxide film occurred on glass substrate (14).The crystallite size D in nm for a known X- ray wavelength λ at the diffraction angle θ of Ag and Ag_2O nanostructures was calculated by using Scherrer formula(1)

$$D = K\lambda/\beta \cos\theta \quad \text{.....1}$$

Where: β is a full width half maximum to this wavelength and from eqs. 2, 3 a strain value 'η' and dislocation density 'δ' of Ag and Ag_2O nanostructures films can be evaluated and listed in Table. 2 (15,16).

$$\eta = \frac{\beta \cos\theta}{4} \quad \text{.....2}$$

$$\delta = \frac{1}{D^2} \quad \text{.....3}$$

These values were varied from 2.601to $2.805*10^{-4}$ lines^{+2} m^{-4} and 3.55-2.38 10^{-4} lines^{-2} m^{-4} respectively, while the dislocation density of the same films were varied from (3.136 to 3.652) 10^{-14} line m^{-2} and 2.356-2.649 10^{-14} line m^{-2}. The results revealed that the strain and dislocation density are decreased with the increasing of the grain size (16).

Table 2. The XRD results of Ag thin films and Ag_2O nanostructured films.

Thin films prepared	(2Θ)° degree	η* 10^{-4} line^{+2} m^{-4}	δ*10^{14} Line m^{-2}	d (Å) XRD	(h k l) plane	FWHM XRD	D(nm)	(2Θ)° ASTM	d (Å) ASTM	Type	Card number
at room temperature	38.0689	2.601	3.136	2.36195	(111)	0.38630	21.6352	38.116	2.3590	Ag	04-0783
	44.2318	3.520	6.282	2.04608	(200)	0.62020	13.7593	44.277	2.0440	Ag	04-0783
	64.4079	2.805	3.652	1.44540	(220)	0.48640	19.3071	64.426	1.4450	Ag	04-0783
T=400 °C 125 nm and 95 s.	32.7824	3.553	2.356	2.69185	(111)	0.30341	27.1466	32.790	2.7290	Ag_2O	41.1104
	38.6156	2.383	2.649	2.28388	(101)	0.33431	24.6223	38.609	2.3300	Ag_2O	19-1155

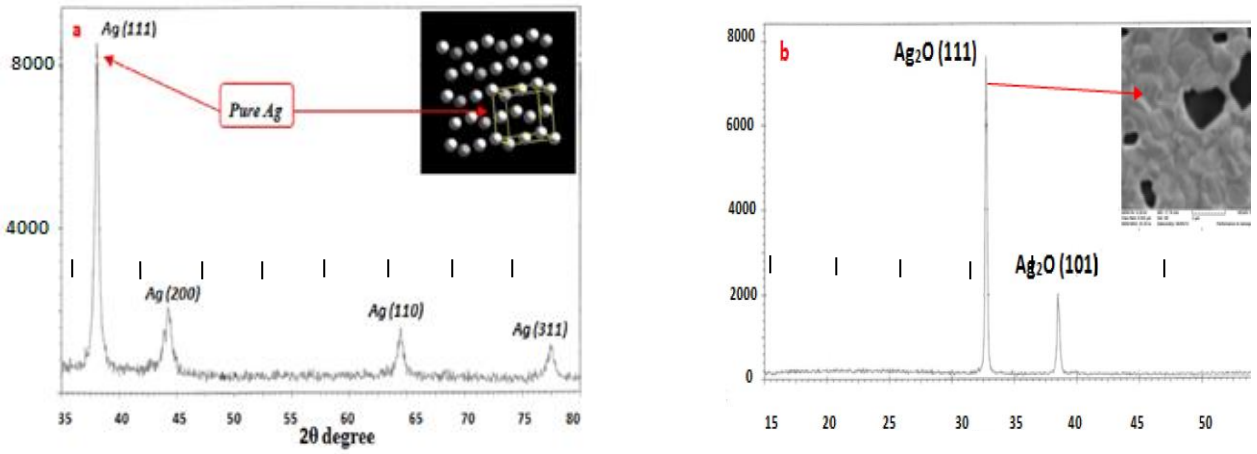

Figure 2. XRD pattern for (a) Ag film and (b) Ag_2O nanostructures film (T=400 °C, 125 nm and 95 s)

Optical Studies of Ag_2O Thin Film

As observed in other works (17, 18), the deposited structure of Ag film on glass substrate without oxygen pressure represents a purely metal film that has high reflectivities in the visible region**.** The film conversion from metal to diaphanous oxide due to the optical quality and crystallinity after treatment oxygen pressure can be greatly improved. As shown in Fig. 3-a which displays the absorption as a function of the wavelength (200-1000) nm, it is known that the sharp increasing of in absorption of Ag_2O film in UV and IR regions is due to the fundamental light absorption and by free-carrier absorption, consecutive this result is conditional with many other works (19, 20**)**.

To date, the spectra of the optical absorption coefficient can be tested by using the next eqs. (11):

$\alpha h\upsilon = A(h\upsilon - Eg)\ m$ for $h\upsilon > Eg$

$\alpha h\upsilon = 0$ for $h\upsilon < Eg$

Where α is the absorption coefficient, A is a constant depending on specifics of the band structure, $h\upsilon$ is the photon energy, Eg is the absorption band gap, m = 2 mentions an allowed indirect transition and m = 1/2 mentions an allowed direct transition. The direct optical band gap was predestined by extrapolating the straight line of $(\alpha h\upsilon)^{1/2}$contra the photon energy as shown in Fig.3-b and it is found to be 1.93 eV and this agrees with the result in a similar work(11).

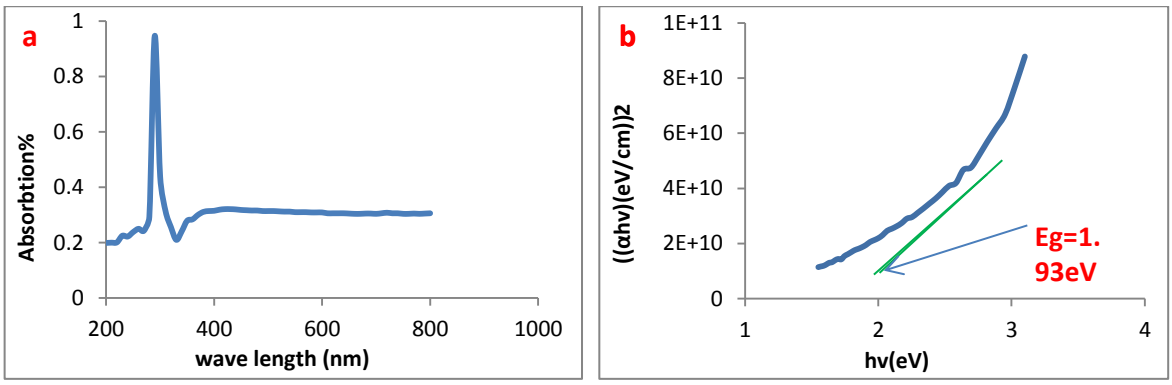

Figure 3. (a) Absorbance curve and (b) Band gap values of Ag_2O thin films

Morphology Studies of Ag_2O Nanocrystals

Figure .4 depicts the SEM images of 125nm as a thick of Ag_2O nanocrystals deposited on n-type, p-type and PS (porous silicon), respectively. Figure 4-b shows that the accumulation of the stars-like are semi-regular of the Ag_2O nanocrystals on the surface of p-type PS and the other diffuse inside the pores in a nearly uniform distribution with a different grain size on the surface and the particles which have size less than the pore size diffuse inside the pores. This accumulation in p-type PS may be attributed to the flow current where charge carriers regularly make much better
etching process than disordered matrix surrounding the nanocrystals of n-type PS as shown in Fig.4-a.Thus, the average quantum efficiency of a p-type PS layer results from a statistical distribution of high quantum efficiency nanocrystals (21).

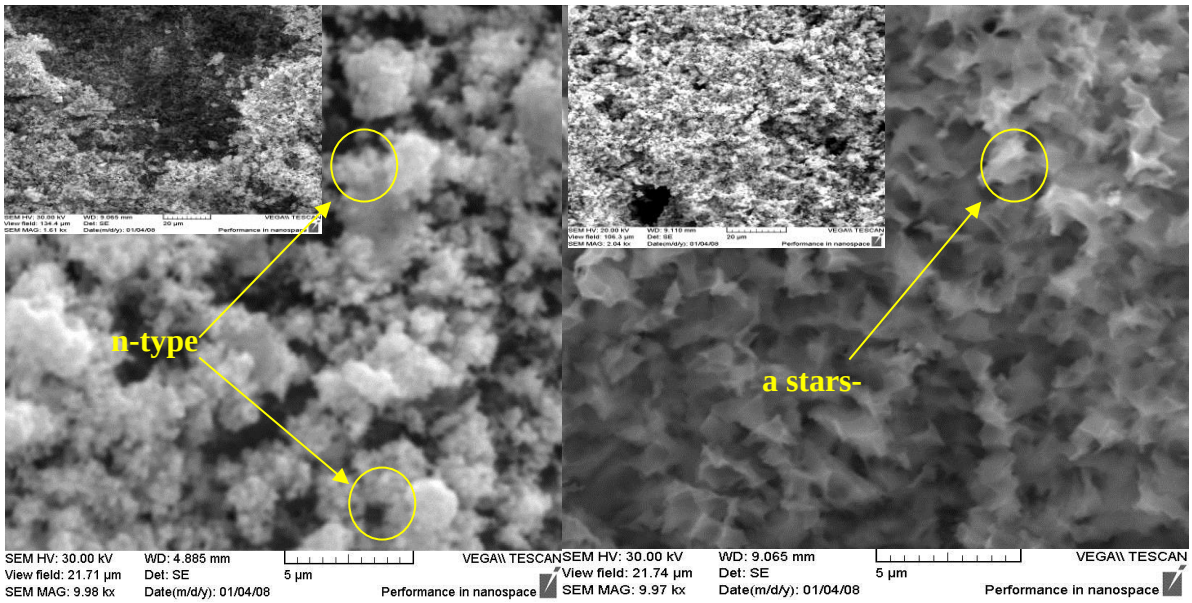

Figure 4. SEM images of Ag_2O nanocrystalline thin films deposited at room temperature and prepared with 23mA/cm^2 Current density was applied for 15min etching time,(a) n-type PS,(b) p-type PS.

Spectral Responsivity

Figure 5 shows the responsivity (R_λ) variation with the wavelength of (p-Ag_2O/n-Si), (p-Ag_2O/p-Si), (p-Ag_2O/PS/n-Si) and (p-Ag_2O/PS/p-Si) Photo detectors respectively, synthesized at 15 min as an etching time and 23 mA/cm^2 as a current density. It can be observed from the Figure that the maximum responsivity exists at visible region and the other at the NIR region , the spectral responsivity detour of these photo detector consists of two response peaks; the first located at 560 nm due to the absorption verge of (Ag_2O/PS) Photo detector pertain. This pertain is very close to the surface and it can reveal short wavelengths (<600 nm). The second peak is located at (750 and 800 nm) due to absorption edge of (n-PS/Si), (p-PS/Si) hetero junctions respectively to reveal the NIR wavelengths (absorption of Si). From Fig. 5 it is evident that the value of responsivity has increased characteristically after the drilling process of p-type (Si) and the maximum value obtained after etching current density of 23 mA/cm^2 was nearly(0.17 A/W) at (λ =800 nm).While the responsivityrate of(n-PSi/Si)

photo detector reachs to about (0.15 A/W). The improvement of responsivity ofAg_2O/p-PS/Si photo detectors can be justified as a result of the partial dissolution of silicon which causes i) the performance of small Si nano crystals in the PS material,(ii) an increased light extraction efficiency from PS,(iii) decreasing the dark current (iiii) increasing the depletion width iiiii) increasing the light absorption(22).

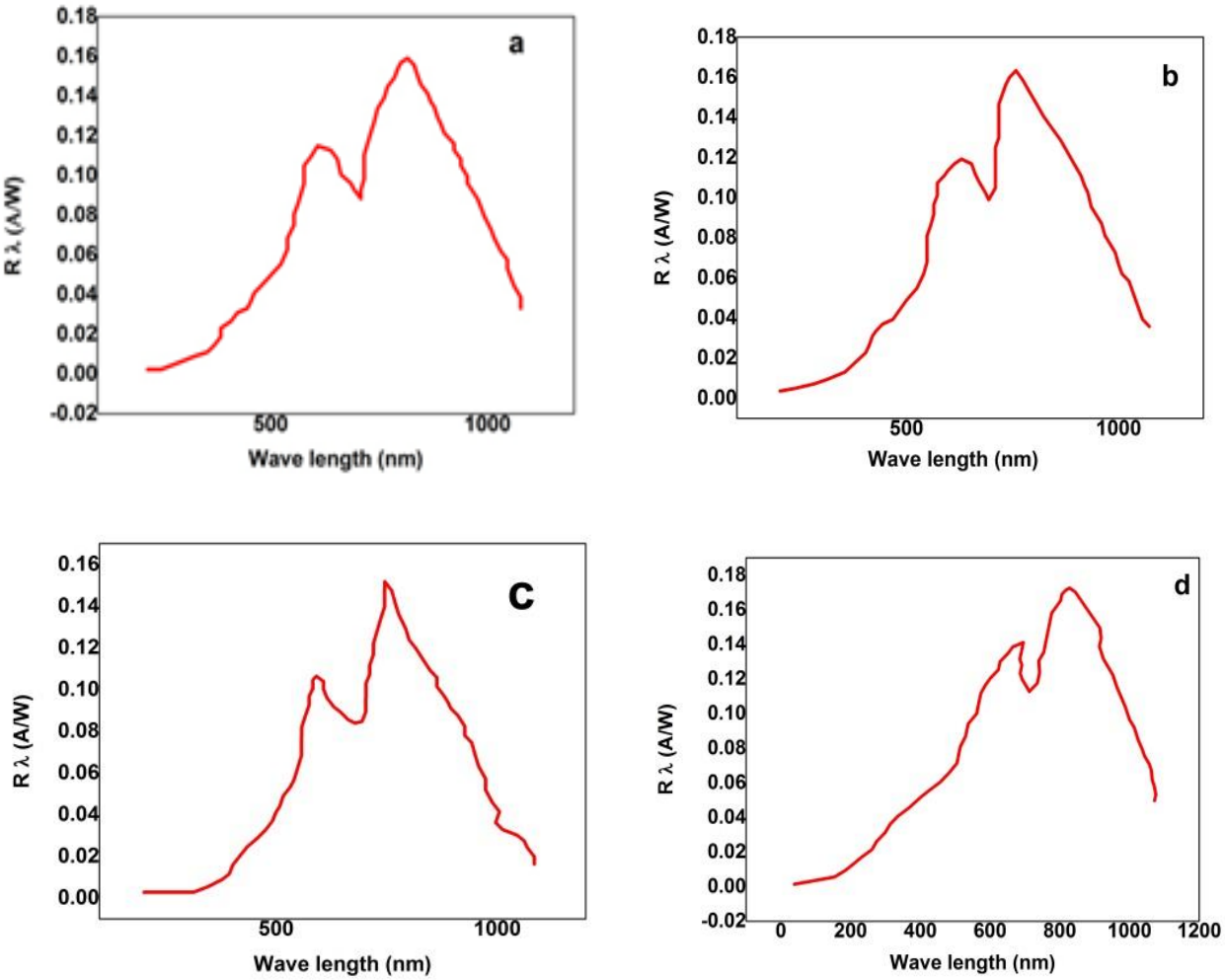

Figure5. Spectral Responsivity plots for a) p-Ag_2O/n-Si, b) p-Ag_2O/p-Si, c) p-Ag_2O/n-PS/Si and d) p-Ag_2O/p-PS/Si, photodetectors.

Specific Detectivity

Figure 6 shows the specific detectivity (D^*) versus the wavelength for (p-Ag_2O/n-Si), (p-Ag_2O/p-Si), (p-Ag_2O/n-PS/Si) and(p-Ag_2O/p-PS/Si) photo detectors, respectively, prepared at the same etching current density, specific detectivity depending directly on responsivity. The maximum detectivity was $5.7*10^{11}$ $W^{-1}cm\ Hz^{1/2}$ at λ = 825 nm and this value increased to $10*10^{11}$ $W^{-1}cm\ Hz^{1/2}$ after the drilling process for n-PS and the maximum $D^*$for p- Si was $8*10^{11}$ $W^{-1}cm\ Hz^{1/2}$ at λ = 775 nm and this value increased to $9.1*10^{11}$ $W^{-1}cm\ Hz^{1/2}$for p-PS (23), this Figure is very important for IR detection since the noise current is very significant**.**

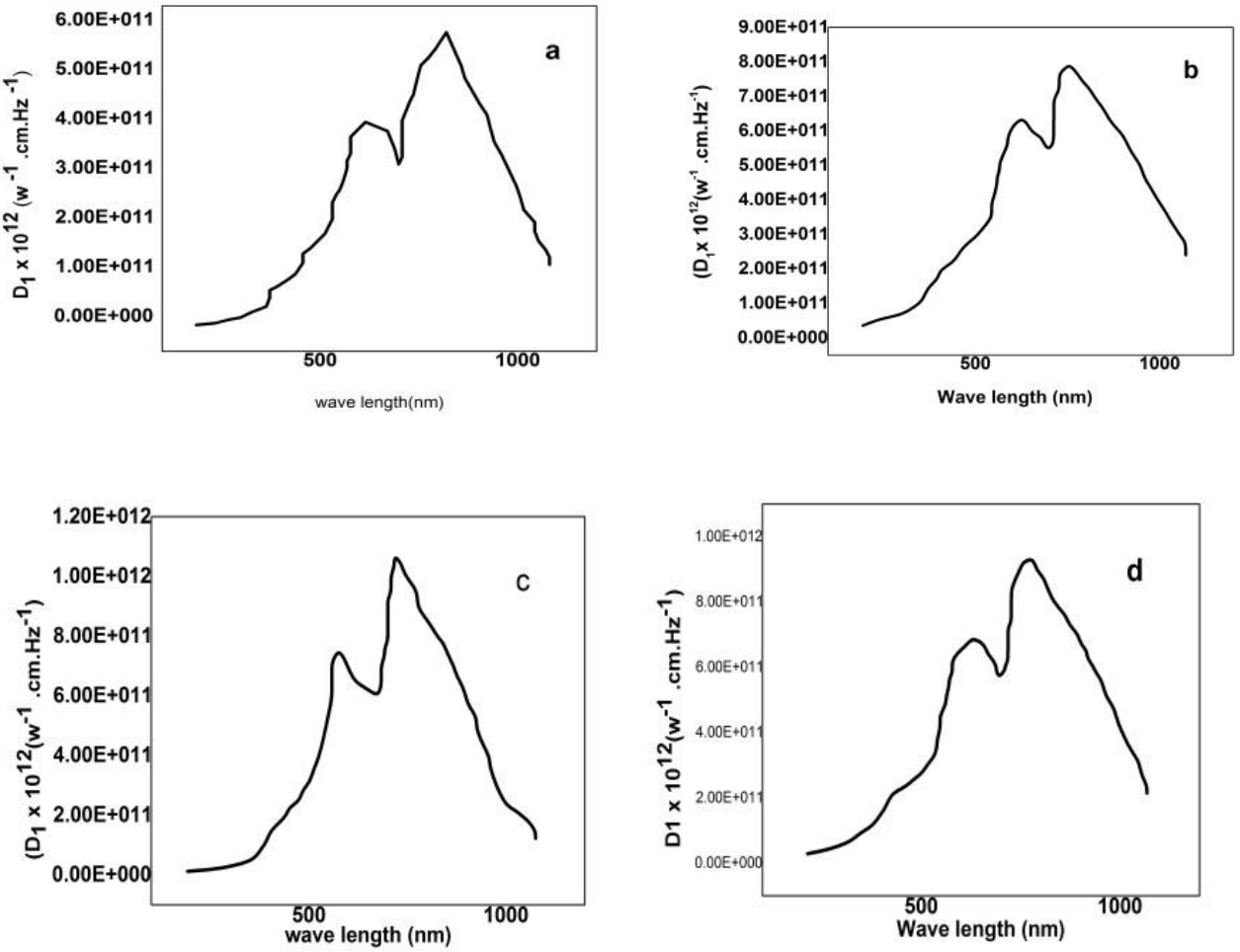

Figure 6. Detectivity depicts of (a) p-Ag_2O/n-Si, (b) p-Ag_2O/p-Si, (c) p-Ag_2O/n-PS/Si and (d) p-Ag_2O/p-PS/Si, photodetectors.

Conclusions:

Silver oxide thin film (high purity oxide) was formed by Thermal Oxidation and the optical properties revealed that the direct band gap of 1.93eV measured by optical absorption experiments for Ag_2O thin film was predestined and indicated to the effect of quantum size. X-ray diffraction measurement disclosed that the Ag_2O film at (400^oC) and (95 s) condition has apyramid - like crystal structure and the reflection was from (111). Scanning electron microscopy (SEM) demonstrated that the Ag_2O/PS nanocrystals prepared by electrochemical etching and photo electrochemical etching processes that can give us advantageous properties of PS and that they are so important to give suspensions photodetector characteristics after deposition of Ag_2O nanostructure. The spectral response (R_λ) and the specific detectivity (D^*) of our photodetectors has been synthesized by the absorption edge of Ag_2O and silicon, respectively.

Conflicts of Interest: None.

References:

1. Hassan MA, Agool IR, Raoof LM. Silver Oxide Nanostructured Prepared on Porous Silicon for Optoelectronic Application. Appl Nanosci. 2014 April;4(4):429–447.
2. Saroja G, Vasu V, Nagarani1 N. Optical Studies of Ag_2O Thin Film Prepared by Electron Beam Evaporation Method. O J Metal.2013 December;(3):57-63.
3. Kavitha P, Suseela S, Mary M. Synthesis and Characterization of Cadmium Sulfide Nanoparticles. Int J Eng Sci.2013 March;2(3):108-110.
4. Reidy B, Haase A, Luch A, Dawson K A, Lynch I. Mechanisms of Silver Nanoparticle Release, Transformation and Toxicity: A Critical Review of Current Knowledge and Recommendations for Future Studies and Applications. Materials. 2013 June; 6(6):2295-2350.
5. Bocka FX, Christensenb TM, Riversc SB, Doucettea LD, Lad R J. Growth And Structure of Silver And Silver Oxide Thin Films On Sapphire. Thin Solid Films. 2004 December;468(2-1):57– 64.
6. Qingyong T, Daxin S, Yaowu S. CuO And Ag_2O/CuO Catalyzed Oxidation of Aldehydes to The

Corresponding Carboxylic Acids by Molecular Oxygen. Molecules. 2008 April;13(4):948-957.
7. Khaldun AS, Hassan Z, Khalid O. Effect of Silicon Porosity on Solar Cell Efficiency. Int J Electrochem Sci. 2012 January;(7) :376 – 386.
8. Raid AI, Alwan M , Ahmed S. Preparation and characteristics study of nano-porous silicon UV photodetector. Appl Nanosci. 2017 February; 7(1–2): 9–15.
9. Salman M. Study of Some optical properties of silver oxide (Ag2O) using UV Visible spectrophotometer. IOSR-JAP. 2016 December;8(6):51-54.
10. Abd Al – Majed AM. Studying the optical and electrical properties Of Cu_2O and Bi_2O_3 films prepared by rapid thermal oxidation: A thesis for Msc Degree. Iraq: College of Science Al-Mustansiriyaih University; 2005.
11. Ismail RA, Habubi NF, Abd AN. Morphological, Structural and Chemical Properties of p-type Porous Silicon Produced by Electrochemical Etching. Int. J. Thin Film Sci. Tec..2015Septemer;121-128.
12. International centre for diffraction data-JCPDS;1998.USA card No. 77-2307.
13. Weifeng W, Xuhui M, Luis AO. Oriented Silver oxide Nanostructures Synthesized Through a Template-Free Electrochemical Route. Int J Mate Chem. 2011 September;(2): 432–438.
14. Raoof LM. Fabricationand characterization of Ag_2O/Si andAg_2O/Psi Heterojunction devices. A Thesis in MSc degree. College of Science Al-Mustansiriyah University .Iraq. 2013.
15. Chate PA, Sathe DJ, Hankare PP. Electrical and crystallographicproperties of nanocrystalline $CdSe_{0.5}S_{0.5}$ composite thin films deposited by dip method. J. Mater. Sci. Mater. Electron. 2011Febarury;22(2):111–115.
16. Abd AN, Habubi NF, Ismail RA. Preparation of colloidal cadmium selenide nanoparticles by pulsed laser ablation in methanol and toluene J. Mater. Sci. Mater. Electron. 2014 July; 25(7):3190–3194.
17. Chawla AK, Singhal S, Gupta HO, Chandra R. Effect of Sputtering Gas on Structural and Optical Properties of Nanocrystalline Tungsten Oxide Films. Thin Solid Films.2008 December; 517(3): 1042-1046.
18. Yi C. Fabrication And Nonlinear Optical Properties Of Nanoparticle Silver Oxide Films. J Appl phys. 2003 July; 94(3): 10.1063/1.1589178.
19. Yong XG. Liang HF. Yuan Z. Effect of the Oxygen Flux Ratio on The Structural and The Optical Properties of Silver-Oxide Films Deposited by Using the Direct-Current Reactive Magnetron Sputtering Method. J. Korean Phys. Soc.2011 February;58(2): 243-247.
20. Swanepoel R. Determination of the Thickness and Optical Constants of Amorphous Silicon .J Phys E .November:16(12). 1214.
21. Gaburro Z, Daldosso N, Pavesi L. Porous Silicon. via Sommarive 14, 1-38050 Povo (Trento), Italy, email:gaburro@science. unitn.it.
22. Abdul Majeed AM. Fabrication and Study the Characterization of Doped SnO_2 /Porous Silicon Heterojunction. A Thesis for the Degree of Doctor. Mustansiriyah University College of Science; 2013.
23. Muhsien MA, Hamdan H. Preparation and Characterization of p- Ag_2O/n-Si Heterojunction devices produced by rapid thermal oxidation. Energy Prodedia. 2012; 18: 300-300-311.

الخواص البصرية والتركيبية لأغشية (Ag_2O/Si & Psi) النانوية لتطبيقات الكواشف البصرية

انتصار عباس حمد[1] رنا اسماعيل خليل[2] اسماء محمد رؤوف[3]

[1]قسم الفيزياء، كلية العلوم للبنات، جامعة بغداد، بغداد، العراق
[2]قسم الفيزياء، كلية العلوم، الجامعة المستنصرية، بغداد، العراق
[3]قسم الفيزياء، كلية التربية، الجامعة المستنصرية، بغداد، العراق

الخلاصة:

اظهر غشاء اوكسيد الفضة نوع القابل (p-type) توصيلية عالية وفجوة طاقة بصرية مباشرة قيمتها 1.93eV,علما ان فجوة الطاقة لغشاء اوكسيد الفضة (Ag_2O) تعتمد وبشكل كبير على طريقة التحضير (التبخير الحراري للفضة بالفراغ ومن ثم الاكسدة الحرارية بدرجة 400 درجة سيليزية وبزمن 95 ثانية). ان الخصائص البصرية لاغشية اوكسيد الفضة تتأثر بشروط الترسيب، اذ تم ترسيب اغشية Ag_2O بسمك 125± على نوعين من السليكون المانح والقابل والمستعمل كقاعدة بصورته العادية مرة ومرة اخرى بصورة مسامية (منمشة) ومن ثم تم فحص حيود الاشعة السينية والفحوصات البصرية للنماذج وفحص المجهر الالكتروني حيث حقق الكاشف الضوئي (P-Ag_2O/P-PSi/Si) اعلى استجابية ضوئية عند القمتين (600 nm) و (800 nm) على التوالي مقارنة مع الكواشف الثلاثة الاخرى، وكان ثابت الشبيكة للفضة المتعددة التبلورعند القمم (111),(200),(110), (311) هو 4.077 A^o ، اظهرت النتائج ان زيادة الحجم الحبيبي تسبب التناقص بقيمة الاجهادات وكثافة الانخلاع . كما اظهرت زيادة حادة في مخطط طول موجة الامتصاص في المنطقة فوق البنفسجية وتحت الحمراء وكذلك تراكم نجمي شبه منتظم لبلورات اوكسيد الفضة النانوية موزعة على سطع العينة المسامية نوع (P) وانتشار اخر داخل المسام بتوزيع منتظم ايضاً وبحجم حبيبي مختلف.كما اظهرت النتائج نقصان كثافة الانخلاعات والمطاوعة بزيادة الحجم الحبيبي.

الكلمات المفتاحية: اوكسيد الفضة، السيليكون المسامي، دراسة تركيبية، الاستجابية الطيفية ، نظام التبخير الحراري بالفراغ .